Supplemental Methods

Reagents, chemicals, and kits

Biotin (Millipore Sigma, PHR1233), chloroquine (Selleckchem, S6999), concanavilin A (Vector Labs, B1005-5), cycloheximide (Millipore Sigma, C4859), L-glutamine (Fisher Scientific, 25030081), IRDye 800CW streptavidin (LI-COR Bio, 926-32230), IL3 (mouse recombinant, carrier-free. BioLegend, 575504), MG132 (Selleckchem, S2619), MEM non-essential amino acids solution (Thermo Fisher, 11360070), Protein G Dynabeads™ (Thermo Fisher, 10004D), sodium pyruvate (Thermo Fisher, 11360070), TRIzol™ Reagent (Thermo Fisher, 15596018), polyethylenimine (PolySCIENCES, 23966-1), ubiquitylation kit (Enzo Life Sciences, BML-UW9920-0001).

Constructs

For stable and transient overexpression, OSTM1-3X-Flag and PDE3B-6X-His were cloned into pLV-EF1a-IRES-Neo (Plasmid #85139 in Addgene). For mouse and human OSTM1 and PDE3B genes CRISPR/Cas9 based knockout, pLenti-CRISPR-V2-puro plasmids with cloned sgRNAs were ordered from Genscript (2 guides/gene/organism). hOSTM1 (guide 1, 5'-TGAACATCACTCGAAAACTA-3'; guide 2, 5'-CTGCTTTGAACATAACCTTC-3'), hPDE3B (guide 1, 5'-TACTGACTATCCCGAAGCAA-3'; guide 2, 5'-TACTGACTATCCCGAAGCAA-3'), mOstm1 (guide 1, 5'-TCGATGCACAAGTGCGTCTC-3'; guide 2, 5'-GCTATTGCAGAATACCTCCG-3') mPde3b (guide 1, 5'-GCTAAATGAAGCTCGCAATA-3'; guide 2, 5'-GGGATCGCAGCAGTGGTAAG-3'). His-ubiquitin, HA-ubiquitin, and Flag-BirA-OSTM1 were cloned into LPC vector. All plasmids were purified using Plasmid Maxi Kit (Qiagen, 12163) and confirmed by Sanger sequencing at GeneWiz.

Lentivirus generation and infection

For lentivirus generation to stably overexpress or knockout our genes of interest, psPAX2 (packaging plasmid), pVSVG (envelope vector) and target plasmids (pLV-EF1a-IRES-Neo/Puro or pLenti-CRISPR-V2-puro) were transfected into HEK293T cells at 3 (PSPAX2): 1 (pVSVG): 4 (target plasmid) ratio using polyethylenimine (PEI) transfection method at 1 (DNA): 3 (PEI) ratio. After overnight incubation, media were changed to fresh media and 48 h later supernatant was collected to infect target cells at $1x10^6$ cells/well density with 5 μg/ml polybrene in 12-well plate. Plate was centrifuged at 193 x g for 2 h at room temperature, then incubated overnight in CO_2

incubator. Culture media were then changed back to fresh media for respective cell lines, followed by antibiotic selection or cell growth measurement.

Cell proliferation assay

Cells were seeded at different densities (Ba/F3 1,000, SU-DHL-5 1,000, OPM2 2,000, Z-138 2,000, RPMI-8226 1,000, ARH-77 1,000, OCI-LY-4 5,000, OCI-LY-7 3,000, OCI-LY-18 2,000, U2932 1,000, SU-DHL-10 1,000, and NALM6 2,000 cells per well) in 96-well plates. Cell number was recorded each subsequent day using Celigo High Throughput Micro-Well Image Cytometer (NEXCELOM Bioscience, Art nr: 200-BFFL-5C-AUTO) until maximum confluence was reached. Fold change in cell number was calculated by normalizing the cell count of each day to that of day 0.

Drug treatments for co-IP and IB

Cells (both adherent and suspension) were treated with MG132 (10 μM or dose response) or chloroquine (100 μM) for the indicated time points. Following treatment, cells were collected for co-immunoprecipitation (co-IP) and/or immunoblotting (IB).

Cell growth, proliferation, and viability assays

Cell growth and proliferation were assessed by daily cell counting. Equal number of cells between tests and controls were seeded in 96-well plates. Cell numbers were quantified daily using a Celigo cell counter. Relative growth was determined by normalizing the reading of cells plated at time 0. Proliferation curves were plotted in GraphPad Prism 8.

Cell viability was measured by Trypan blue (MPBio, 23966-100) exclusion method. Cells were seeded at equal densities and treated as indicated. At specified time points, cells were collected, mixed 1:1 with 0.4% Trypan blue solution, and counted using an automated cell counter. Viable (Trypan blue–negative) and nonviable (Trypan blue–positive) cells were quantified, and percent cell death was calculated relative to untreated controls. For time-course experiments, viable cell numbers were normalized to day 0 and vehicle-treated controls as indicated.

For all cell growth and viability assays, 3-5 replicates for each sample were performed.

Ubiquitylation assay in cultured cells

Non-denaturing IP-ubiquitylation detection

Stable OSTM1-Flag or PDE3B-His overexpressing (Ba/F3 or BCL cell lines) or transiently transfected (using PEI method) HEK293T cells were lysed in IP lysis buffer, and 500 µg protein lysate was incubated with Protein G beads and respective antibodies at 4˚C overnight. For endogenous PDE3B pull down, PDE3B-ab was used. For cells overexpressing PDE3B-His, 6x-His tag antibody was used. Beads were separated by magnetic separation and washed 2x with wash buffer 1, 2x with wash buffer 2 and once with IP lysis buffer. Bound PDE3B was eluted with 1x Laemmli buffer, followed by IB with ubiquitin antibody.

High-denaturing IP-ubiquitylation detection

1×10^6 HEK293T cells were plated into 6-cm petri dish. After overnight attachment, cells were transfected with 2 µg HA-Ub, 2 µg PDE3B-His, and 2 µg OSTM1-Flag constructs using PEI transfection. Cells were harvested 48 h after transfection. One tenth of cells were lysed in RIPA buffer and the remaining cells were dissolved in Buffer A (6 M guanidine-HCl, 0.1 M Na_2HPO_4/NaH_2PO_4, 10 mM imidazole, pH8.0) and sonicated. Each sample was added with 50 µl PureCube Ni-NTA MagBeads (Cube Biotech, 31205) equilibrated with Buffer A and incubated for 3 h at room temperature on rotation. The agarose beads were precipitated by centrifugation and washed once with Buffer A, twice with Buffer B (10 mM Tris-Cl, pH 8.0, 8 M urea, 0.1 M NaH_2PO_4) and three times with 1:4 diluted Buffer B supplied with 25 mM imidazole. The precipitates were resuspended in 100 µl 2X Laemmli buffer (4% SDS, 20% glycerol, 10% β-mercaptoethanol, 0.004% bromophenol blue, 0.125 M Tris HCl pH 6.8) with 200 mM imidazole, boiled at 95℃ for 10 min and subjected to IB.

Cancer Cell Line Encyclopedia (CCLE) data analysis

CRISPR-Cas9 gene dependency (Chronos Gene Effect) and protein abundance data for OSTM1 and PDE3B were obtained from the CCLE database (DepMap Public 23Q4+ release; https://depmap.org/portal/). Gene effect scores were used to assess dependency across BCL cell lines and visualized as bar graphs in Graphpad Prism 8.

Protein abundance data, expressed as relative abundance normalized to the bridge sample, were available for a subset of BCL cell lines. Pearson correlation between protein abundances of OSTM1 and PDE3B was calculated in Microsoft Excel, and correlations were visualized as scatter plots in GraphPad Prism 8.

Publicly available patient data analysis

Copy number analysis

For *OSTM1*, *CDKN2A,* and *PDE3B* copy number analysis across B-cell malignancies, two datasets were available in cBioPortal: DLBCL (Lymphoid Neoplasm Diffuse Large B-cell Lymphoma (TCGA, Firehose Legacy) with an n=48 and Mature B-cell malignancies (MD Anderson Cancer Center) with 752 patients spread across different B-cell lymphoma subtypes such as DLBCL, MCL, FL, BL, MZL, HGBL and CLL). The copy number data was obtained from these datasets to determine the frequency of alterations. Co-alteration analysis was done by making oncoplots using Oncoprinter (https://www.cbioportal.org/oncoprinter).

Furthermore, copy number analysis was also performed for several other publicly available datasets (1) (n=304), multiple myeloma (2) (n=725), B-cell chronic lymphocytic leukemia (3) (n=97), follicular lymphoma (4, 5), plasmablastic lymphoma (6), and Burkitt's lymphoma (7).

Analysis of publicly available GEO datasets

Gene expression datasets relevant to BCL were retrieved from the NCBI Gene Expression Omnibus (GEO). For each dataset, the series matrix file and the corresponding platform annotation file were downloaded. Expression data were aligned to the annotated gene symbols and combined for downstream analyses.

For *OSTM1*, tumor versus normal expression was analyzed using GSE32018, GSE56315, and GSE12195, while survival analyses were performed using GSE10846, GSE181063, GSE4475, GSE119214, and GSE2658. For *PDE3B*, tumor versus normal expression comparisons included GSE2350, GSE56315, GSE12195, and GSE50006, and survival analyses were conducted using GSE4475 and GSE2658.

All analyses were performed using Microsoft Excel. Expression differences between two groups were assessed using Student's *t*-test, and differences among more than two groups using one-way ANOVA. For survival analysis, patients were stratified into high- and low-expression groups based on the median expression of the indicated gene, and survival plots were generated accordingly.

Correlation analysis of CREB1–CREBBP target genes

CREB1 and CREBBP target genes were identified from ChIP–seq datasets available in ChIP-Atlas (CREB1: SRX190216; CREBBP: SRX2339191, SRX2339193, SRX6099462). The top 1,500 genes common across these datasets were selected for further analysis. Their expression patterns were examined in the cBioPortal “Mature B-cell Malignancies (MD Anderson Cancer Center)” dataset. Pearson correlation coefficients between CREB1/CREBBP target genes and OSTM1, PDE3B, and CREB1 expression were calculated in Microsoft Excel. Statistically significant correlations ($p < 0.05$) were visualized using Morpheus, and overlapping gene sets (e.g., PDE3B negatively correlated vs. OSTM1 and CREB1 positively correlated genes) were identified using the Venny tool.

Ba/F3 cell line derived allograft mice

sgControl, sg*Ostm1,* and sg*Ostm1*/sg*Pde3b* Ba/F3 cells were GFP labelled using lentiviral infection. $1x10^6$ GFP labeled cells were resuspended in 500 μl DPBS (Thermo Fisher, 14190250) and injected via intraperitoneal (i.p.) in nude mice. Mice were monitored until the development of tumor related characteristics such as abdominal enlargement and lethargy. At the endpoint, survival span was recorded, mice were euthanized, and secondary lymphoid organs spleen, liver, and lymph-node weights were recorded. Subsequently, tumorigenic organs were crushed, and single cell suspension was prepared in DPBS and analyzed under fluorescent microscope for GFP^+ cells enrichment comparison between sgControl and sg*Ostm1* allografts.

Cycloheximide chase assay

$2x10^6$ cells (ARH-77, Ba/F3, RPMI-8226, and Z-138 cells) were seeded in 12-well plates and treated with 100 μg/ml cycloheximide or DMSO. Cells were collected at different timepoints, washed with DPBS, lysed in 2x Laemmli buffer then subjected to IB.

Tandem mass tag (TMT) proteomics

Cell pellets from sgControl (triplicate) and sg*Ostm1* (triplicate) were used for protein identification and relative quantitation using multiplex TMT approach. Total protein was extracted using lysis buffer containing 8 M urea, 100 mM TEAB and 1X protease inhibitor with sonication. Protein concentration was measured using BCA assay. Fifty microgram total protein from each replicate was reduced by DTT and alkylated by IAM followed by in-solution trypsin digestion. The resulting peptides were labeled with TMT reagents. After the TMT labeling, the peptides from all 6 samples were combined and desalted using C18 cartridge followed by high pH RPLC

separation. A total of 12 fractions were collected and further analyzed by RPLC-MS/MS on an Orbitrap Fusion Lumos Mass Spectrometer using MS2 method. The MS/MS spectra were searched against UniProt mouse database using Sequest search engine on Proteome Discoverer (V2.4) platform. The quantitation comparison was calculated as follows: Ratio (sg*Ostm1*/sgCtrl) = The sum of (each group) TMT abundance/The sum of (sgCtrl) TMT abundance. The proteins with the ratios greater than 1.5-fold and passed the T-Test ($p \leq 0.05$) are considered significantly changed and used for further analysis.

Bio-ID mass spectrometry

Flag-BirA-OSTM1 transiently or stably expressing cells were grown in the presence of 50 μM biotin for 24 h. Cells were harvested and lysed in RIPA buffer (50 mM Tris (pH 7.4), 150 mM NaCl, 1% Triton X-100, 1% sodium deoxycholate, 1% SDS) with sonication. 500 μg of total lysate was incubated with 100 μl avidin beads slurry at 4°C overnight with rotation. Avidin beads were washed twice with wash buffer 1 (2% SDS in dH_2O), once with wash buffer 2 (20 mM Tris, pH 7.4, 500 mM NaCl, 1% Triton X-100, 1 mM EDTA, 1 mM EGTA), once with wash buffer 3 (20 mM Tris, pH 7.4, 300 mM NaCl, 1% Triton X-100, 1 mM EDTA, 1 mM EGTA) and once with wash buffer 4 (20 mM Tris, pH 7.4, 100 mM NaCl, 1% Triton X-100, 1 mM EDTA, 1 mM EGTA). Bound proteins were removed with SDS sample buffer boiling at 95°C for 5 min. Eluates were run on SDS-PAGE, then subjected to IB or mass-spectrometry (MS).

For MS, in-gel trypsin digestion was performed. The resulting peptides were analyzed by LC-MS/MS on Orbitrap Fusion Lumos MS instrument. The MS/MS spectra were searched against Uniprot mouse database using Sequest search engines on Proteome Discoverer (V2.4) platform. The protein false discovery rate is less than 1%. The ratio of Flag-BirA-OSTM1/vector was calculated. The proteins containing more than one unique peptide are identified with more confidence.

RNA extraction, cDNA synthesis, qPCR

RNA of tissue/cell lines was isolated using TRIzol™ Reagent based on manufacturer's guideline. Subsequently, reverse transcription was done using Superscript III First Strand Synthesis system (Invitrogen). qRT-PCR was performed with Power SYBR™ Green PCR Master Mix (Thermo Fisher) on StepOnePlus (applied following primers: mPde3b-F: GCTAAATGAAGCTCGCAATA mPde3b-R: GTGGAGTTGGGAAACTGGT ; mOstm1 (on-site)-F: CGAACTGCGCAAATTGCCT, mOstm1 (on-site)-R: TCGATGCACAAGTGCGTCTC ; hOSTM1

(mRNA expression)-F: AAGATGCAATGAACATCACTCG, hOSTM1 (mRNA expression)-R: GACTTGAGACGTTTGGGCAG ; hOSTM1 gRNA1 (on-site)-F: CTGCTTTGAACATAACCTTCAGGG, hOSTM1 gRNA1 (on-site)-R: GTCACTGCAAGGGACTGAAC; hOSTM1 gRNA2 (on-site)-F: GCCAGAAGTCTCTTAATGGCAGAT, hOSTM1 gRNA2 (on-site)-R: TGTGCATTCCCCTGAAGGTT.

Genomic DNA sequencing for CRISPR knockout validation in cell lines

Genomic DNA (gDNA) was isolated from sgControl and sg*OSTM1* ARH-77 and Ba/F3 cells using QIAamp DNA Mini Kit (Qiagen, 51304). Isolated gDNA was used to setup PCR using primers designed from region flanking gRNA targeting mouse and human OSTM1 for knockout. For Ba/F3 cells, following primer set was used: F: CACGCAGAGATACTGTGTCCA, R: ACAGAGACACCGTAGAGCCT and for ARH-77 cells, following primers were used: F: ACTGTAGTGTGAAACGAAGCTG, R: ACAATCACACACCTCAATCAATGT for amplifying ~0.5 kb size amplicon. The amplicons were used for sanger sequencing using sequencing primer CATACAGTCTCCTCCCACCAAA for Ba/F3 and ATATAAATGACAACATAGAATTGTTC for ARH-77 cells.

Co-immunoprecipitation

Adherent (HEK293T) or suspension (BCL cell lines) cells were collected and centrifuged at 1,000 x g for 3 min. After being washed with cold PBS, cells were lysed in IP lysis buffer (20 mM Tris, pH 7.5, 100 mM NaCl, 1% Triton X-100, 1 mM EDTA, 200 mM PMSF) supplemented with protease inhibitor cocktail on ice for 30 min. The cell lysates were cleared by centrifugation at 4°C to collect supernatant. The supernatant (250-500 μg) was incubated with magnetic beads (Anti-FLAG M2) or Protein G Dynabeads™ with either 6x-His or PDE3B antibodies) overnight at 4°C on rotator. The complexes were precipitated with magnetic stand, and washed twice with IP wash buffer 1 (20 mM Tris, pH 7.5, 300 mM NaCl, 1% Triton X-100, 1 mM EDTA, 200 mM PMSF) in a rotator for 5 min, washed twice with IP wash buffer 2 (20 mM Tris, pH 7.5, 200 mM NaCl, 1% Triton X-100, 1 mM EDTA, 200 mM PMSF) for 5 min, then once with IP lysis buffer for 5 min, and resuspended the complexes with 60 μl IP lysis buffer, boiled in SDS sample buffer at 95°C for 5 min and subjected to IB.

Immunoblotting using cell lysate from cell lines and mouse tissues

Spleen tissues were harvested and snap frozen in liquid nitrogen. Lysates were prepared using homogenization in RIPA buffer with 1% SDS and protease inhibitors cocktail (MCE Chemicals) and quantified using BCA kit (Thermo Fisher, A55864). BSA was used for making standard curves. For cell lines, lysates were prepared in 2X Laemmli sample buffer (1610737EDU) and quantified using Pierce™ 660nm Protein Assay Reagent (Thermo Fisher, 22660) with the addition of Ionic Detergent Compatibility Reagent for Pierce™ 660nm Protein Assay Reagent (Thermo Fisher, 22663). 10-30 µg protein was separated in SDS-PAGE and transferred to nitrocellulose blotting membrane. Primary antibodies were incubated overnight at 4 °C in 5% milk in TBST, and Alexa fluor conjugated secondary antibody was incubated for 1 h at room temperature in 5% milk. Imaging the blot was done using the Odyssey imaging system (LI-COR Biosciences).

Flow cytometry

At endpoint, two femur bones were isolated and separated from attached muscular tissue. The ends were cut and the marrow was flushed in HBSS buffer. Spleen tissue was physically disrupted between frosted slides to get a single cell suspension. Splenocytes were washed with HBSS and subject to ACK (Thermo Fisher, A1049201) lysis to remove RBCs and passed through a 70 µm cell strainer (Fisher Scientific, 22-363-548). 2 x 10^6 cells from bone marrow and splenocytes were blocked with rat serum and FcR blocking antibody 2.4G2 (BioLegend 101302) and incubated with fluorophore conjugated antibodies: Cd3e (BioLegend 100351), B220 (Biolegend 103206), CD19 (BioLegend 115540), CD21/CD35 (BioLegend 123434), CD23 (BioLegend 101621), IgD (BioLegend 405720), IgM (BioLegend 406509), CD38 (BioLegend 102720), CD138 (BioLegend 142534), CD11b (BioLegend 101210), Gr-1 (BioLegend 108456), CD43 (BD Biosciences 740668), CD93 (BioLegend 136503), CD5 (BioLegend 100636), CD95 (BioLegend 152612), GL7 (BioLegend 144614), and PNA (Vector Laboratories FL-1071). Data were acquired on Cytek Aurora Spectral Flow Cytometer (Cytek Biosciences, Fremon, CA) and analyzed on the FlowJo software (TreeStar, San Carlos, CA).

Bulk-RNA sequencing of purified B cells and data analysis

Splenic B cells were purified from WT, *Ostm1*$^{-/-}$, *Cdkn2a*$^{-/-}$ and *Ostm1*$^{-/-}$;*Cdkn2a*$^{-/-}$ (DKO) mice using CD43 negative selection. Briefly, spleen was harvested from mice and single cell suspension was prepared. Red blood cell lysis was done using ACK lysing buffer (Thermo Fisher, A1049201) and the cell suspension was passed through 70 µm strainer (Fisher Scientific, 22-363-548). Splenocytes were incubated with microbeads coated with anti-CD43 antibody (Miltenyi Biotec, 130-

049-801) and passed through LS columns (Miltenyi Biotec, 130-042-401). Resultant eluates containing splenic B cells were counted using trypan blue counting and subjected to RNA isolation. RNA purity was confirmed by running 1% agarose gel.

RNA-sequencing was performed at the University of Texas Health San Antonio (UTHSA) Genome Sequencing Facility. RNA-seq library was prepared with 500 µg of total RNA following the Illumina TruSeq stranded mRNA sample preparation guide. After quantification, the library was subjected to cBot amplification and subsequent 50 bp single read sequencing on the Illumina HiSeq 3000 platform using 100 PE sequencing module.

The RNA-seq reads were mapped to the mouse genome reference (Mus musculus genome (UCSC mm10)) using HISAT2, Gene-level quantification was counted using feature counts, differentially expressed gene analysis was conducted using DEseq, heatmap was generated using iDEP online tool https://bioinformatics.sdstate.edu/idep/. Functional enrichment analysis was performed using the Metascape online tool https://metascape.org/gp/index.html#/main/step1 and KEGG pathway analysis using ShinyGO 0.85 https://bioinformatics.sdstate.edu/go/.

Single-cell RNA sequencing (scRNA-seq)

Cell Isolation

Spleens were harvested from experimental mice and placed in cold DPBS. Tissues were immediately cut in small pieces and then gently pressed through a 100 µm mesh cell strainer using the plunger end of a syringe. Cell suspension was diluted with DPBS and centrifuged at 400 x g for 5 min at 4°C. To eliminate red blood cells, the cell pellet was resuspended in 5 mL of red cell lysing buffer (Roche Diagnostics) and incubated for 3 min at room temperature. Cell suspension was then filtered through a 30 µm mesh cell strainer, diluted with cold DPBS, and centrifuged. After additional washing with DBPS, splenocytes were resuspended in DPBS containing 0.4% (w/v) bovine serum albumin (BSA) (Millipore Sigma) and counted using a hemocytometer with cell viability assessed using Trypan Blue staining. A sample containing 1.5 x 10^6 viable cells/mL was filtered through a 20 µm mesh cell strainer, counted again, and then used for single cell RNA-sequencing. Cell viability for all samples ranged between 80 and 92%.

Library construction and sequencing

Single cell RNA-sequencing was performed by the Stony Brook University/Northport VAMC Single Cell and Spatial Multiomics Facility, using the Chromium Next GEM Single Cell 5' Reagent kit v2,

according to the manufacturer's instructions (10x Genomics, protocol CG000331). Briefly, 10,000 single cells per sample were captured in Gel Bead-In-Emulsions (GEMs) using Chromium iX (10x Genomics). After reverse transcription in a PCR cycler, the barcoded full-length cDNA was purified, amplified with PCR for 11 cycles, and further purified with SPRISelect reagent (Beckman Coulter). Fragment size distribution and quantification of the amplified cDNA were obtained using a Tapestation 4200 (Agilent) with a D5000 High Sensitivity Assay (Agilent).

5' single cell RNA-seq libraries were constructed using 50 ng cDNA. After fragmentation, end-repair, A-tailing and size selection purification, the cDNA was ligated with Illumina adaptors and subsequently purified with SPRISelect reagent. Libraries were amplified and barcoded by PCR with dual index oligonucleotides from the Chromium Dual Index TT Set A kit (10X Genomics), for a total of 16 PCR cycles. The final PCR products were subjected to double-sided size selection with SPRISelect beads (0.6x and 0.8x). The library fragment size distributions were analyzed on an Agilent 4200 Tapestation and a Fragment Analyzer, and library yields and concentrations were determined by qPCR using the KAPA Illumina Library Quantification PCR kit (Roche Diagnostics).

Library sequencing was performed at a depth of ~50,000 paired reads/cell on an Illumina NovaSeq X Plus instrument operated by a commercial provider (Novogene, Inc.), with the following paired-end sequencing settings: Read1, 151 cycles; i7 index, 10 cycles; i5 index, 10 cycles; Read2, 151 cycles.

Data analysis

Raw sequencing reads were processed using Cell Ranger v8.0.1 to generate gene–cell count matrices. Downstream analysis was performed in R v5.3.1 within RStudio. Filtering was done using perCellQCMetrics and perCellQCFilters functions from the Scater package v1.34.1. Cells with total features or counts more than three median absolute deviations (MADs) below the median were discarded, as were cells with mitochondrial transcript percentages more than three MADs above the median. Identification of mitochondrial genes was done using AnnotationHub v3.14.0. Genes expressed in fewer than two cells were also removed. Doublets were removed using DoubletFinder v2.0.6.

Filtered cells were processed and clustered using the standard Seurat v5 workflow, including normalization, scaling, principal component analysis (PCA), and uniform manifold approximation and projection (UMAP). The number of principal components used for UMAP dimensionality

reduction was determined by the minimum between the point where cumulative variance explained exceeded 90% and the variance contribution of the individual PC was less than 5%, and the point where the drop in variance explained between consecutive PCs was less than 0.1%. Cell types were classified with SingleR v2.8.0 by using the ImmGenData reference from the Celldex package v1.16.0. B cells were subset and clustered using FindNeighbors and FindClusters at resolution 0.3. Low-quality B-cell clusters with median counts below 500 and median features below 200 were removed. The remaining B cells were re-clustered at resolution 0.6, and subtypes were identified using common B-cell markers. Differentially expressed genes were found using FindMarkers using the test.use=wilcox_limma argument. Genes meeting the criteria of p value < 0.05 and log2 fold change > 0.5 were included in the over-representation analysis. Over-representation analysis was done using the clusterProfiler package v.4.14.6 and the gene sets used were from the MsigDB website (https://www.gsea-msigdb.org/gsea/msigdb).

Immunohistochemistry (IHC)

IHC and IF were performed as previously described (8). For IHC, after hydration, antigen retrieval was performed in 10 mM citrate buffer (pH 6.0) by heating the section for 10 min and then allow it to sit for 30 min. The endogenous peroxidase activity was quenched in 3% H_2O_2 in MeOH. The section was blocked for 2.5 h with 10% goat serum followed by primary antibody incubation overnight at 4 °C. After washing, the section was incubated with biotinylated secondary antibody for 1 h, then streptavidin-biotin complex (Vectastain Elite ABC kit, Vector Laboratories) was applied for 30 min. Peroxidase substrate solution 3,3′-diaminobenzidine (DAB, Cell Signaling # 8059S) was applied for proper time until desired color reaction is observed. The reaction was terminated by rinsing gently with distilled water. Section was then counterstained with hematoxylin, dehydrated, and coverslipped.

BCR repertoire profiling

Mouse BCR repertoire profiling from total RNA was performed as described (9). In brief, total RNA was isolated from splenocytes and reverse-transcribed into cDNA. Multiplex PCR were used to amplify immunoglobulin (Ig) heavy chain VDJ regions. PCR amplicons were purified using NEBNext Sample Purification Beads and subjected to high-throughput sequencing. Pair-end reads were assembled and UMI-corrected. Bulk IgH repertoire profiling was performed using next-generation sequencing data processed through the Immcantation framework (version 4.4.0). Raw FASTA and IgBLAST output files (.fmt7) were converted into Change-O databases with Change-O v1.3.1 running inside a Conda “immcant” environment (Python 3.10, Bioconda

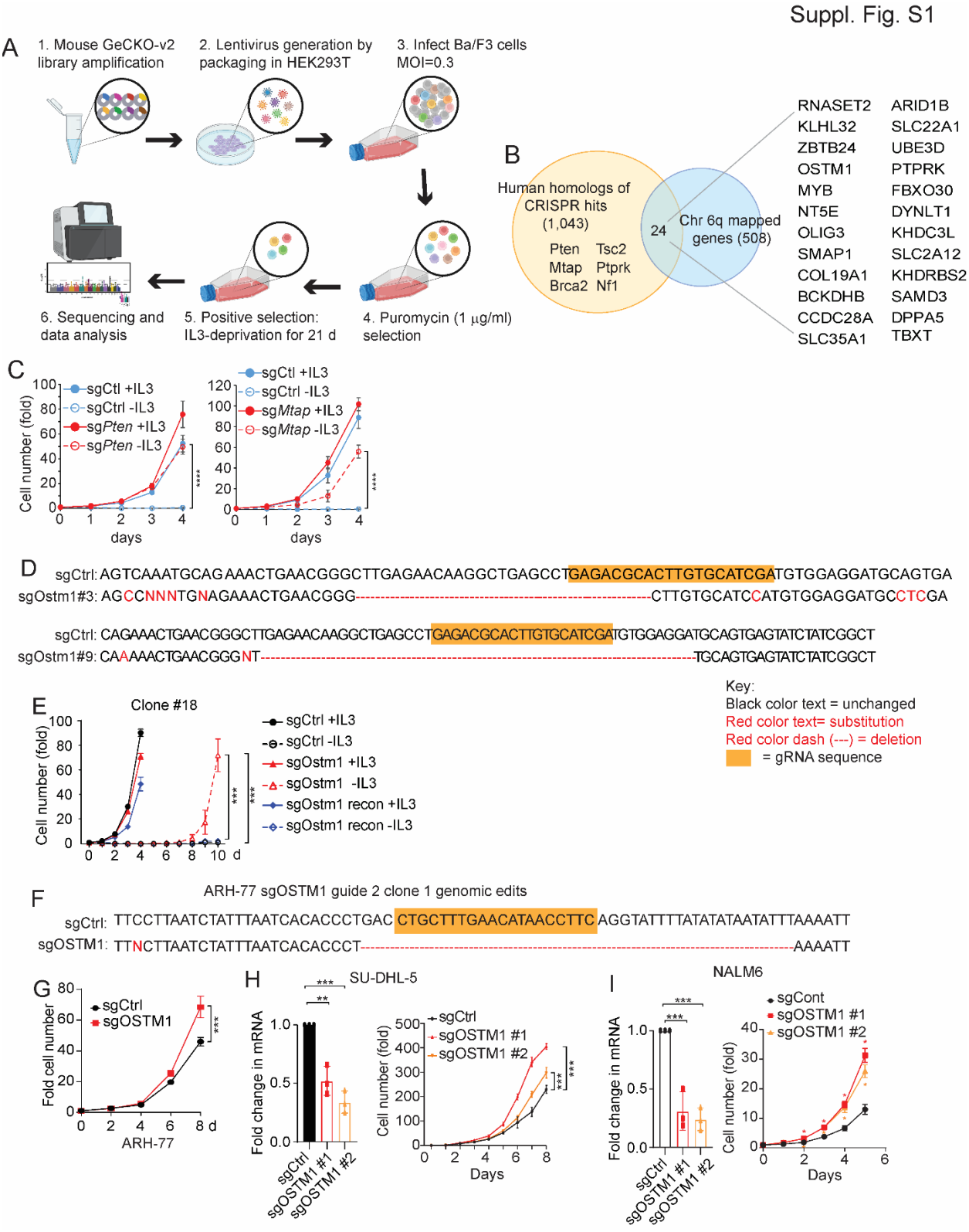
channels). Germline reference sequences for Mus musculus (IGHV, IGHD, IGHJ) were obtained from IMGT/GENE-DB (release 2025-10). IgBLAST v1.22.0 was used for V(D)J alignment with the corresponding IMGT germline database. Productive IGH reads were identified (locus = IGH, productive = True), and clonal clustering was performed using a Hamming-distance model (--model ham, --dist 0.15, --norm len, --act set) to group sequences sharing identical V and J genes and CDR3 length within a normalized junction distance $\leqslant$15% normalized Hamming distance across the junction region to account for somatic hypermutation. Downstream tabulation and visualization were done in Python 3.10 using pandas v2.2 and matplotlib v3.8. Constant-region (C-gene) assignments (c_call) were derived from IgBLAST to determine isotype usage. Clonal frequencies were expressed as the fraction of total unique molecular identifier (UMI)-normalized sequences per sample (10).

References

1. Chapuy B, Stewart C, Dunford AJ, Kim J, Kamburov A, Redd RA, et al. Molecular subtypes of diffuse large B cell lymphoma are associated with distinct pathogenic mechanisms and outcomes. *Nat Med*. 2018;24(5):679–90.
2. Hoang PH, Cornish AJ, Sherborne AL, Chubb D, Kimber S, Jackson G, et al. An enhanced genetic model of relapsed IGH-translocated multiple myeloma evolutionary dynamics. *Blood Cancer J*. 2020;10(10):101.
3. Parry EM, Leshchiner I, Guieze R, Johnson C, Tausch E, Parikh SA, et al. Evolutionary history of transformation from chronic lymphocytic leukemia to Richter syndrome. *Nat Med*. 2023;29(1):158–69.
4. Oricchio E, Nanjangud G, Wolfe AL, Schatz JH, Mavrakis KJ, Jiang M, et al. The Eph-receptor A7 is a soluble tumor suppressor for follicular lymphoma. *Cell*. 2011;147(3):554–64.
5. Kalmbach S, Grau M, Zapukhlyak M, Leich E, Jurinovic V, Hoster E, et al. Novel insights into the pathogenesis of follicular lymphoma by molecular profiling of localized and systemic disease forms. *Leukemia*. 2023;37(10):2058–65.
6. Frontzek F, Staiger AM, Wullenkord R, Grau M, Zapukhlyak M, Kurz KS, et al. Molecular profiling of EBV associated diffuse large B-cell lymphoma. *Leukemia*. 2023;37(3):670–9.
7. Burkhardt B, Michgehl U, Rohde J, Erdmann T, Berning P, Reutter K, et al. Clinical relevance of molecular characteristics in Burkitt lymphoma differs according to age. *Nat Commun*. 2022;13(1):3881.
8. Bott AJ, Shen J, Tonelli C, Zhan L, Sivaram N, Jiang YP, et al. Glutamine Anabolism Plays a Critical Role in Pancreatic Cancer by Coupling Carbon and Nitrogen Metabolism. *Cell Rep*. 2019;29(5):1287–98 e6.
9. Werner A, Schafer S, Gleussner N, Nimmerjahn F, and Winkler TH. Determining immunoglobulin-specific B cell receptor repertoire of murine splenocytes by next-generation sequencing. *STAR Protoc*. 2022;3(2):101277.
10. Jung J, Zhu S, Lalani A, Shakarchi J, Matracz B, Wu GG, et al. Commensal Bacteria Drive B-cell Lymphomagenesis in the Setting of Innate Immunodeficiency. *Blood Cancer Discov*. 2025;6(5):505–25.

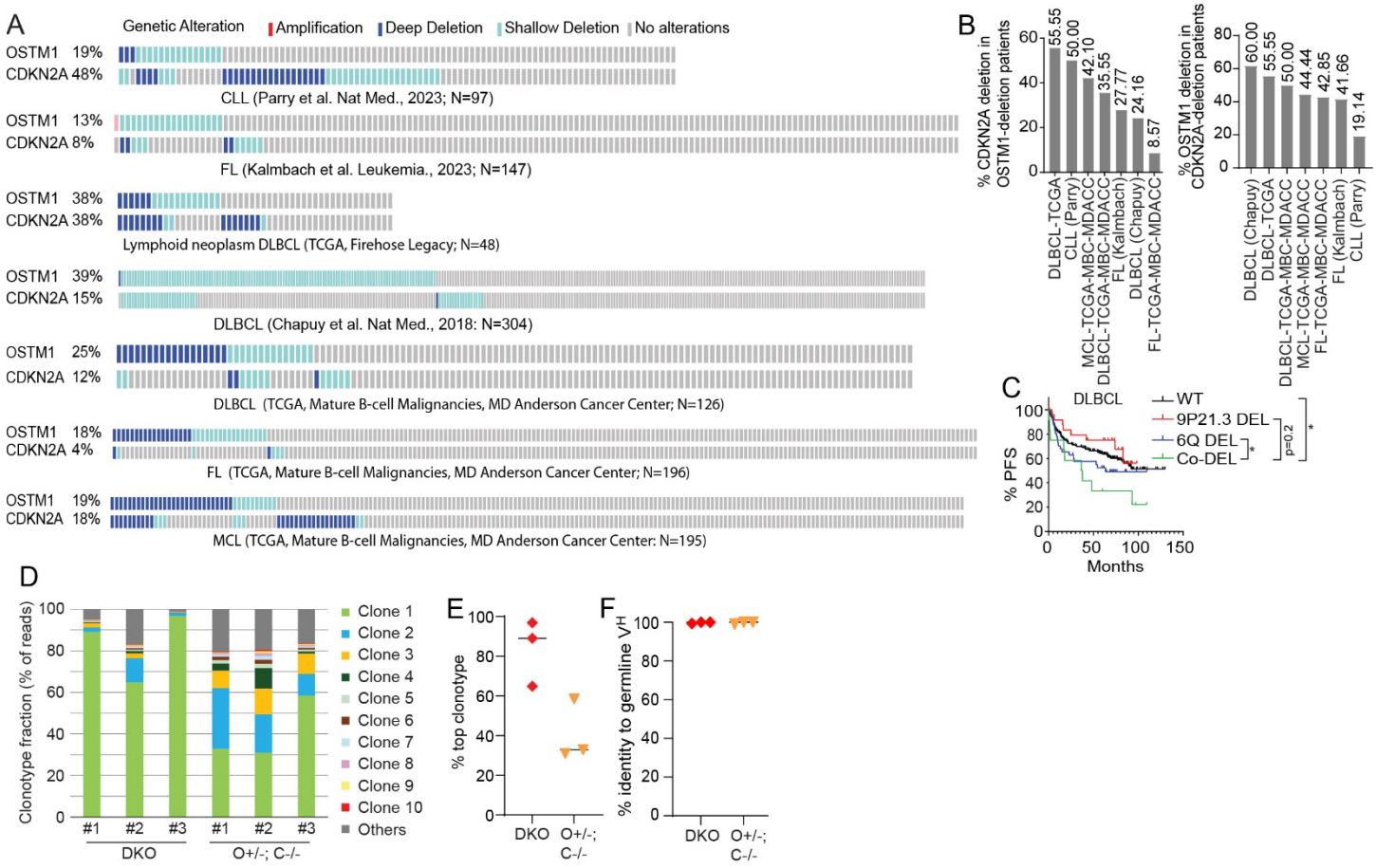
Supplemental Figures

Suppl. Fig. S1



Supplemental Figure S1 (related to Figure 1). (A) Workflow of the CRISPR/Cas9 screen in Ba/F3 cells. **(B)** Venn diagram depicting the overlap between CRISPR hits with human homologs (1,043) and genes mapped to chr. 6q (508). **(C)** Ba/F3 cells stably expressing sgPTEN and sgMTAP became IL3-independent. ****p<0.0001 (Repeated-measures ANOVA in R). **(D)** Ostm1 was silenced in Ba/F3 cells using two independent sgRNAs. Successful knockout of Ostm1 was determined by genomic sequencing, which shows frame-shifting deletion, point mutations, and large-size deletion. **(E)** Human OSTM1-Flag was reconstituted into sg*Ostm1* Ba/F3 cells, which led to the loss of IL3-independence of the sg*Ostm1* cells. **(F)** OSTM1 was silenced in ARH-77 cells using sgRNA. Successful knockout of OSTM1 was determined by genomic sequencing. **(G)** Silencing OSTM1 in ARH-77 cells promoted cell proliferation. **(H and I)** OSTM1 was silenced in DLBCL cell line SU-DHL-5 **(H)** and B-ALL cell line NALM6 **(I)** with two sgRNAs. Successful silencing was achieved indicated by decreased mRNA levels, which led to increased cell proliferation. Statistical analysis of the survival curves in panels **E**, **G**, **H,** and **I** was done using multiple t-test, one per row. For bar graphs in panels **H** and **I**, one way ANOVA was used. **p<0.01; ***p<0.001.

Suppl. Fig. S2



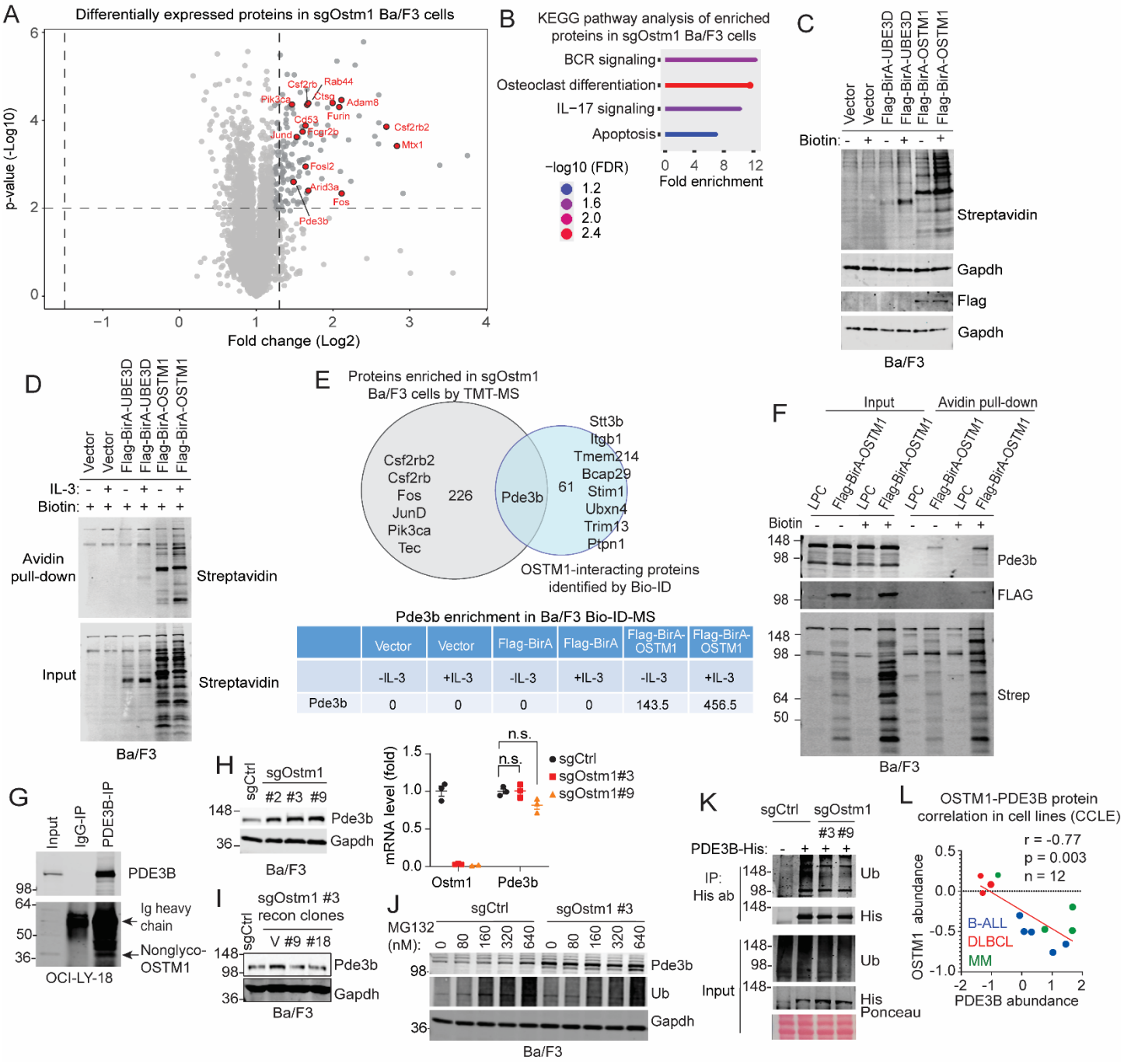
Supplemental Figure S2 (related to Figure 3). (A) Oncoprint visualization of *OSTM1* and *CDKN2A* co-deletions across different BCLs as reported in the indicated studies. **(B)** Frequencies of *CDKN2A* deletions among patients with *OSTM1* deletions across BCLs (left), and the frequencies of *OSTM1* deletion among patients with *CDKN2A* deletions (right), in the indicated studies. **(C)** Progression-free survival of DLBCL patients (1) stratified by the presence of chr. 6q deletion (*OSTM1* DEL), 9p21.3 deletion (*CDKN2A* DEL), both (*Co-DEL*), or neither (WT). Patients with co-deletions had worse survival. (**D**) Frequencies of individual clonotypes obtained from Igh V(D)J sequencing of mouse spleen samples. Each clonotype is color-coded according to its rank of prevalence within the corresponding sample. (**E**) Comparison of the frequency of the most expanded clonotype across samples, grouped by genotype. (**F**) Percent identity between BCL Igh V(D)J sequences and their corresponding germline sequences, grouped by genotype.

Suppl. Fig. S3


A
DKO 4491
DKO 4531
Receipient nude mice
Spleen
LN
BM
B
BM
LMC-WT
O-/-
B220+CD19+
B220+CD19+ IgM+CD43-
B220+CD19+ IgM+CD43- B220low/int CD93+
B220+CD19+ IgM+CD43- B220hi CD93-
C
% of B220+CD19- in BM cells
% of B220+CD19+ B-lineage cells
% of Pro-B in B220+CD19+
% of Pre-B in B220+CD19+
% of immature B in B220+CD19+
% of recirculating mature B in B220+CD19+
BM cell number (x10⁶)
Number of B220+CD19+ cells in BM (x10⁶)
Number of pro-B cells in BM (x10⁶)
Number of pre-B cells in BM (x10⁶)
Number of inmature B cells in BM (x10⁶)
Number of mature B cells in BM (x10⁶)
D
Spleen
Young adult
Mid -aged
Splenocyte number (x10⁶)
% of splenic B cells
Splenic B cell number (x10⁶)
% of FO B in splenic B cells
% of MZ B in splenic B cells
E
Spleen
Naïve
SRBC-immunized
B220+ gated B cells
F
SRBC-immunized
Splenocyte number (x10⁶)
% of splenic B cells
Splenic B cell number (x10⁶)
% of GC B in splenic B cells
Number of splenic GC B-cells (x10⁶)

Supplemental Figure S3 (related to Figure 3). Characterization of splenocyte transplantation, and B-cell development and germinal center responses in *Cd19*-Cre driven *Ostm1*$^{-/-}$ (O$^{-/-}$) mice. (A) Representative transplantation of DKO splenic BCL into nude recipient mice. Splenocytes (1x10^6) isolated from DKO mice (ID: 4491 or 4531) were injected intraperitoneally (i.p.) into each nude recipient mouse. At 7-9 weeks post-transplantation, the spleen, LN, and BM cells were harvested and analyzed by flow cytometry (FACS). FACS profiles of primary DKO splenocytes are shown for comparison. **(B)** Representative flow cytometric profiles of bone marrow (BM) cells from naïve adult mice (27-36 weeks old) stained to identify B-lineage cell subsets. Gated populations were defined as follows: early B-lineage-enriched cells, B220$^+$CD19$^-$CD43$^+$sIgM$^-$; pro-B cells, B220$^+$CD19$^+$CD43$^+$sIgM$^-$; pre-B cells, B220$^+$CD19$^+$CD43$^-$sIgM$^-$; immature B cells, B220low/intCD19$^+$CD43$^-$sIgM$^+$CD93$^+$IgD$^-$CD23$^-$; transitional-like BM B cells, B220intCD19$^+$sIgM$^+$CD93$^+$IgD$^+$CD23$^+$; and recirculating mature B cells, B220highCD19$^+$sIgM$^+$CD93$^-$IgDhighCD23$^+$. **(C)** Summary graphs showing the frequencies and absolute numbers of the indicated B-lineage subsets in the BM, as determined by flow cytometry. **(D)** Summary graphs showing the frequencies and absolute numbers of splenic B-cell subsets in naïve young adult (8-18 weeks old) and mid-aged (27-36 weeks old) mice, as determined by flow cytometry. Gated populations were defined as follows: total B cells, B220$^+$CD3$^-$; follicular (FO) B cells, B220$^+$CD3$^-$CD23$^+$CD21int; and marginal zone (MZ) B cells, B220$^+$CD3$^-$CD23intCD21$^+$. **(E)** Representative flow cytometric profiles of splenocytes stained to identify germinal center (GC) B cells in naïve and sheep red blood cell (SRBC)-immunized mice. For immunization, mice were injected intraperitoneally (i.p.) with 10% SRBCs in PBS, and splenocytes were analyzed by flow cytometry on day 10 after immunization. GC B cells were defined as B220$^+$CD3$^-$GL7$^+$CD95$^+$PNA$^+$. **(F)** Summary graphs showing the frequencies and absolute numbers of total splenic B cells and GC B cells, as determined by flow cytometry. *P* values for comparisons between the two genotypes in B, C, and E were determined using an unpaired Student's *t* test. ns, not significant.

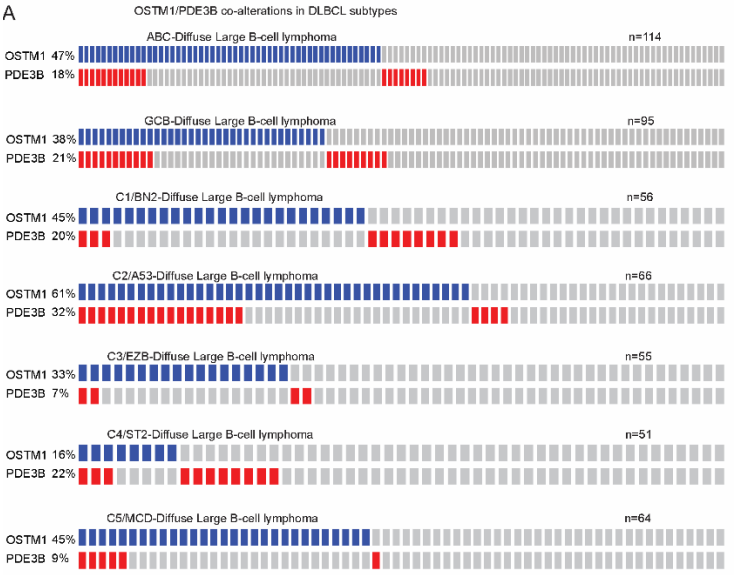
Suppl. Fig. S4



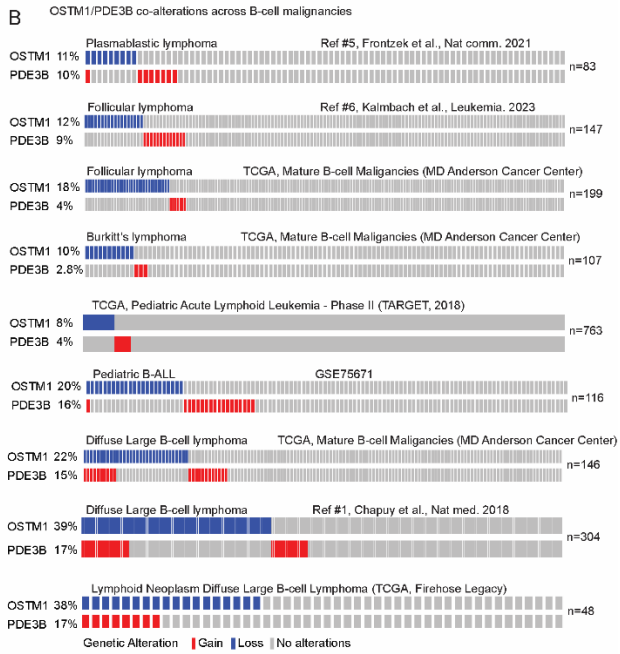
Supplemental Figure S4 (related to Figure 4). (A) sg*Ostm1* and sgControl Ba/F3 cells were subjected to TMT-MS. Volcano plot (log_2 fold change vs. $–log_{10}$ p-value) was generated using VolcaNoseR. Dashed lines indicate significance cutoffs. Selected proteins involved in hematopoeitic function and differentiation are highlighted in red. **(B)** KEGG pathway enrichment

analysis of proteins involved in sg*Ostm1* Ba/F3 cells with -log10(FDR) used as the significance metric. **(C)** Flag-BirA-OSTM1 was stably expressed in Ba/F3 cells. 50 μM biotin was added to the cells for 24 h. Cells were lysed in BioID lysis buffer and the BirA activity was confirmed by HRP-conjugated streptavidin in IB. Successful expression of Flag-BirA-OSTM1 was confirmed by Flag IB. The lanes showing Flag-BirA-UBE3D were for a different project. **(D)** Ba/F3 cells stably expressing Flag-BirA-OSTM1 were cultured in the absence or presence of IL3. Biotin was added to the cell lysates. Avidin pull-down was performed and probed for streptavidin by IB. Biotinolyted proteins were detected. **(E)** Venn diagram depicting the overlap between proteins enriched in sg*Ostm1* cells identified by TMT-MS and OSTM1-interacting partners identified by BioID in Ba/F3 cells. The table shows BioID enrichment scores for Pde3b. **(F)** Avidin beads pull-down was performed on Ba/F3 cells expressing Flag-BirA-OSTM1, followed by IB with the indicated antibodies. Note that Pde3b was detected to interact with Flag-BirA-OSTM1. **(G)** OSTM1 interacts with PDE3B at the endogenous level. Endogenous PDE3B was immunoprecipitated from OCI-LY-18 lysates with PDE3B antibody or IgG as isotype control. Subsequently, IB was performed using PDE3B and OSTM1 antibodies. **(H)** *Ostm1* was silenced in Ba/F3 cells, and three independent cell clones were probed for Pde3b by IB (left). qRT-PCR analysis of sg*Ostm1* cell clones showing that Pde3b mRNA levels were not affected by *Ostm1* silencing (right). **(I)** OSTM1-Flag was stably reconstituted in sg*Ostm1* Ba/F3 cell clone #3, and Pde3b was probed by IB. **(J)** sgControl and sg*Ostm1* Ba/F3 cells were treated with indicated concenrations of MG132 for 8 h, and Pde3b was detected by IB. **(K)** PDE3B-His was expressed in sgControl or sg*Ostm1* Ba/F3 cells. IP with PDE3B antibody was performed, followed by IB with indicated antibodies. PDE3B-His ubiquitination was detected in sgControl cells and reduced in sg*Ostm1* cells. **(L)** Spearman correlation analysis of OSTM1 and PDE3B protein abundance across BCL cell lines from different subtypes using CCLE proteomic data.

Suppl. FIg. S5



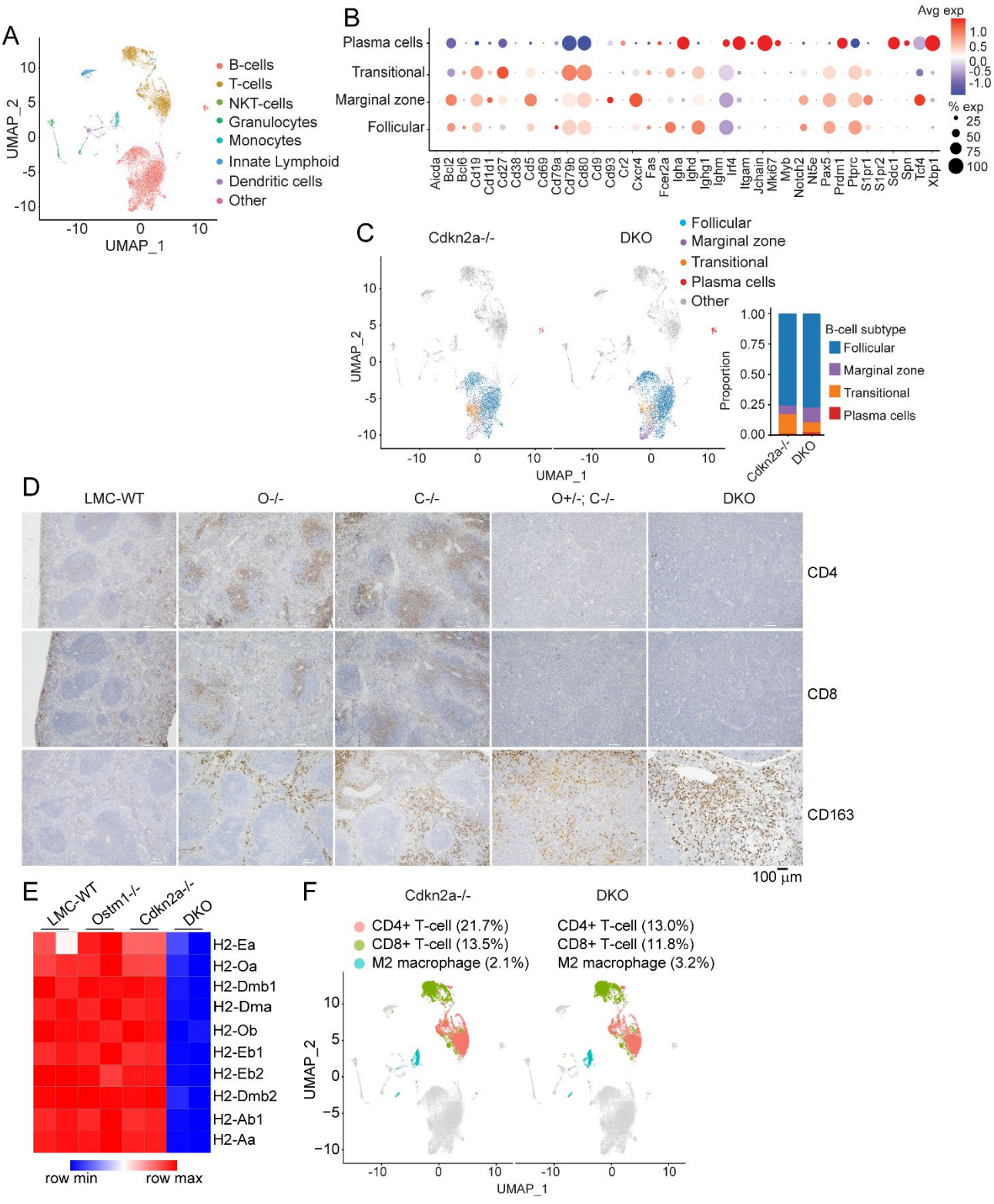
	ABC	GCB	C1/BN2	C2/A53	C3/EZB	C4/ST2	C5/MCD
Total number of patients	114	95	56	66	55	51	64
Total number of patients with PDE3B gains	21	20	11	21	4	11	6
Total number of patients with OSTM1 deletions	53	36	25	40	18	8	29
Total number of patients with co-alteration	12	11	3	17	2	3	5
% PDE3B gains in OSTM1 deletion patients	57	55	27	81	50	27	17
% OSTM1 deletions in PDE3B gain patients	22	30	12	42	11	37	83



Supplemental Figure S5 (Related to Figure 5). OSTM1-PDE3B co-alterations across DLBCL subtypes and B-cell malignancies.

(A) OncoPrint of *OSTM1* and *PDE3B* copy-number alterations across the seven DLBCL subtypes (ABC, GCB, C1/BN2, C2/A53, C3/EZB, C4/ST2, and C5/MCD) (1). Each column represents an individual patient; red indicates PDE3B copy-number gain, blue indicates OSTM1 loss, and grey indicates no alterations. The percentage of patients with *OSTM1* loss and *PDE3B* gain is shown at left for each subtype and cohort size (n) at right. The accompanying table summarizes, for each subtype, the total number of patients, the number with *PDE3B* gain, the number with *OSTM1* loss, the number with co-alteration (*OSTM1* loss and *PDE3B* gain), and the resulting proportions, showing that a substantial fraction of *OSTM1*-deleted tumors also harbor *PDE3B* gain (up to 81% in the C2/A53 subtype). **(B)** OncoPrints of *OSTM1* and *PDE3B* copy-number alterations across B-cell malignancies subtypes, as indicated from the published datasets and cohorts indicated above each panel (1, 5, 6). Across independent studies and disease types, *OSTM1* loss and *PDE3B* gain recurrently co-occur the most in DLBCL.

Suppl. Fig. S6


A
B-cells
T-cells
NKT-cells
Granulocytes
Monocytes
Innate Lymphoid
Dendritic cells
Other
UMAP_1
UMAP_2
B
Plasma cells
Transitional
Marginal zone
Follicular
Avg exp
% exp
Aicda Bcl2 Bcl6 Cd19 Cd1d1 Cd27 Cd38 Cd5 Cd69 Cd79a Cd79b Cd80 Cd9 Cd93 Cr2 Cxcr4 Fas Fcer2a Igha Ighd Ighg1 Ighm Irf4 Itgam Jchain Mki67 Myb Notch2 Nt5e Pax5 Prdm1 Ptprc S1pr1 S1pr2 Sdc1 Spn Tcf4 Xbp1
C
Cdkn2a-/-
DKO
Follicular
Marginal zone
Transitional
Plasma cells
Other
Proportion
B-cell subtype
D
LMC-WT
O-/-
C-/-
O+/-; C-/-
DKO
CD4
CD8
CD163
100 µm
E
LMC-WT
Ostm1-/-
Cdkn2a-/-
DKO
H2-Ea
H2-Oa
H2-Dmb1
H2-Dma
H2-Ob
H2-Eb1
H2-Eb2
H2-Dmb2
H2-Ab1
H2-Aa
row min
row max
F
Cdkn2a-/-
DKO
CD4+ T-cell (21.7%)
CD8+ T-cell (13.5%)
M2 macrophage (2.1%)
CD4+ T-cell (13.0%)
CD8+ T-cell (11.8%)
M2 macrophage (3.2%)

Supplemental Figure S6 (Related to Figure 6). (A) Spleens from two-month-old $C^{-/-}$ and DKO mice were harvested for scRNA-seq. Pan-cell-type UMAP embeddings with cells from both $C^{-/-}$ and DKO mice combined (n=10,000 cells per mouse) are shown. **(B)** Dot-plot of B-cell markers stratified by sub-population is shown. Color represents average log fold expression. **(C)** UMAP plots of B-cell subpopulations are shown by genotype. Bar graphs show the relative proportions. **(D)** IHC of spleens harvested at the end-point of DKO mice. Representative CD4, CD8, and CD163 IHC images are shown. $CD4^+$ and $CD8^+$ T-cell staining was reduced, while $CD163^+$ M2-like macrophage staining was increased in $O^{+/-};C^{-/-}$ and DKO spleens. Scale bar, 100 μm. **(E)** Heatmap of MHC class II gene expression from bulk RNA-seq of purified splenic B cells of the indicated genotypes, showing marked suppression of MHC class II genes in DKO B cells relative to other genotypes. Rows represent individual genes; color indicates row-normalized expression (row min to row max). **(F)** Spleens from two-month-old $C^{-/-}$ and DKO mice were harvested and 10,000 cells per mouse were analyzed by single-cell RNA-seq. UMAP plots show $CD4^+$ and $CD8^+$ T-cell, and M2-macrophage populations by genotype, with the fraction of each population indicated. DKO mice show reduced $CD4^+$ and $CD8^+$ T-cell fractions and an increased M2 macrophage fraction relative to $C^{-/-}$ mice.